

Supplementary Information

Numerical estimation of drug loading contents in amphiphilic nanogels

Ante Markovina^{1,†}, Clara López Iglesias^{1,2,†}, Ruiguang Cui,¹ Daniel Klinger^{1,*}

¹*Freie Universität Berlin, Institute of Pharmacy, Königin-Luise Straße 2–4, 14195 Berlin, Germany*

²*Department of Pharmacology, Pharmacy and Pharmaceutical Technology, I+D Farma group (GI-1645), Faculty of Pharmacy, Instituto de Materiales (iMATUS) and Health Research Institute of Santiago de Compostela (IDIS), Universidade de Santiago de Compostela, Campus Vida s/n, 15782 Santiago de Compostela, Spain*

† Equal contribution

E-Mail: daniel.klinger@fu-berlin.de

Table of contents

1. Developing a library of amphiphilic nanogels with hydrophobic cargos	3
1.1. Synthesis of nanogels with varying network hydrophobicity	3
1.1.1. Attenuated total reflectance – Fourier transform infrared spectroscopy (ATR-FTIR) of the NGs library.	3
1.1.2. Transmission electron microscopy (TEM) of the NGs library.....	5
1.1.3. Dynamic light scattering (DLS) of the NGs library	6
1.2. Loading of amphiphilic nanogels with hydrophobic cargos.....	7
1.2.1. Calibration curves from UV/Vis spectrophotometry for the cargo library	7
1.2.2. Calibration curves from HPLC measurements for the cargo library.....	10
2. Calculating solubility parameters for amphiphilic nanogels and cargos.....	12
2.1. Determination of Hansen solubility parameters (HSPs) for amphiphilic nanogels.....	12
2.2. Determination of Hansen solubility parameters for drugs and dyes	17
2.3. Calculation of Hildebrand solubility parameters.....	25
2.3.1. Cohesive energies, molar volumes and Hildebrand solubility parameters for amphiphilic nanogels	25
2.3.2. Cohesive energies and molar volumes for drugs and dyes	26
3. PART A – Numerical parameters for ANG-cargo interactions: Combining CHOLA-20 particles with library of different cargos.....	26
3.1. Calculation of Flory-Huggins interaction parameters and optimization of α -values	26

3.2. Correlating Flory-Huggins parameters from HVK method with experimental loading contents	29
3.3. Calculation of Hildebrand solubility parameters	29
3.4. Correlating Hildebrand solubility parameters with experimental loading contents	30
3.5. Calculation of the distance of Hansen solubility parameters R_a	31
3.6. Correlating R_a with experimental loading contents	31
4. PART B - Influence of the type of hydrophobic groups on the correlation between numerical parameters and cargo loading contents	32
4.1. Calculation of Flory-Huggins parameters and R_a values for the combination of amphiphilic nanogels with coumarin, curcumin and Nile red	32
4.2. Influence of hydrophobic structure on the correlation between Flory-Huggins interaction parameters (calculated by HVK method) and cargo LC	33
4.3. Influence of hydrophobic structure on the correlation between R_a and cargo LC (comparison of HVK and YMB method).....	34
5. PART C - Influence of hydrophobic content on the correlation between numerical parameters and cargo LC	35
5.1. Calculation of Flory-Huggins parameters and R_a values for the combination of amphiphilic nanogels with coumarin, curcumin and Nile red	35
5.2. Influence of hydrophobic content on the correlation between Flory-Huggins interaction parameters (calculated by HVK method) and cargo LC	36
5.3 Influence of hydrophobic content on the correlation between R_a and cargo LC (comparison of HVK and YMB method).....	37
6. Part D: Integrating all correlations into a master curve as predictive model for cargo loading in amphiphilic nanogels	38
7. References.....	39

1. Developing a library of amphiphilic nanogels with hydrophobic cargos

1.1. Synthesis of nanogels with varying network hydrophobicity

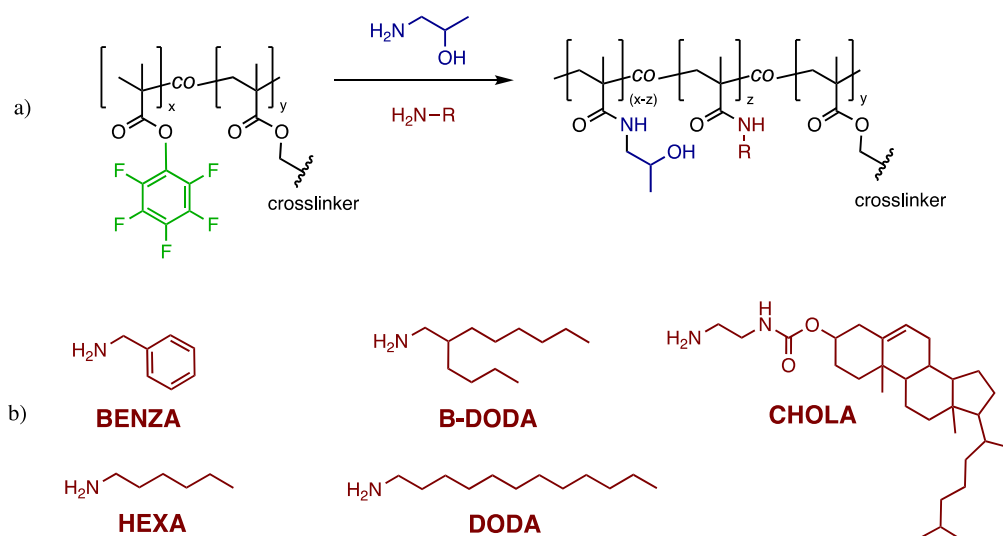


Figure S1. General reaction scheme for the synthesis of amphiphilic nanogels (ANGs): functionalization of reactive precursor particles (a) with different hydrophobic groups (b).

1.1.1. Attenuated total reflectance – Fourier transform infrared spectroscopy (ATR-FTIR) of the NGs library.

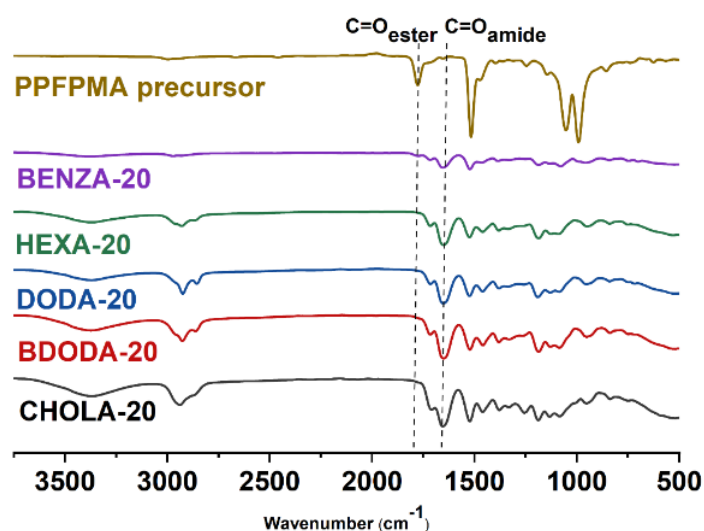


Figure S2. ATR-FTIR spectra show successful network functionalization of the amphiphilic NGs library with 20 mol-% of different hydrophobic groups. Functionalization was confirmed by observing the disappearance of the peak at 1775 cm^{-1} (PFP ester bond of the precursors) and the simultaneous appearance of a functionalized amide bond peak at 1655 cm^{-1} .

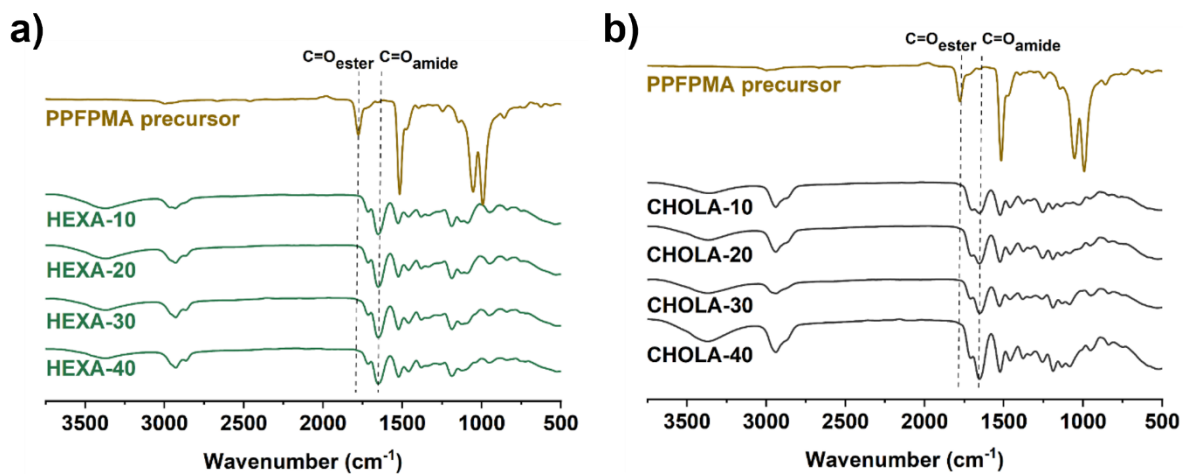


Figure S3. ATR-FTIR spectra show successful network functionalization of the amphiphilic NGs library with varying contents of HEXA (a) and CHOLA (b) groups. Functionalization was confirmed by observing the disappearance of the peak at 1775 cm^{-1} (PFP ester bond of the precursors) and the simultaneous appearance of a functionalized amide bond peak at 1655 cm^{-1} .

1.1.2. Transmission electron microscopy (TEM) of the NGs library

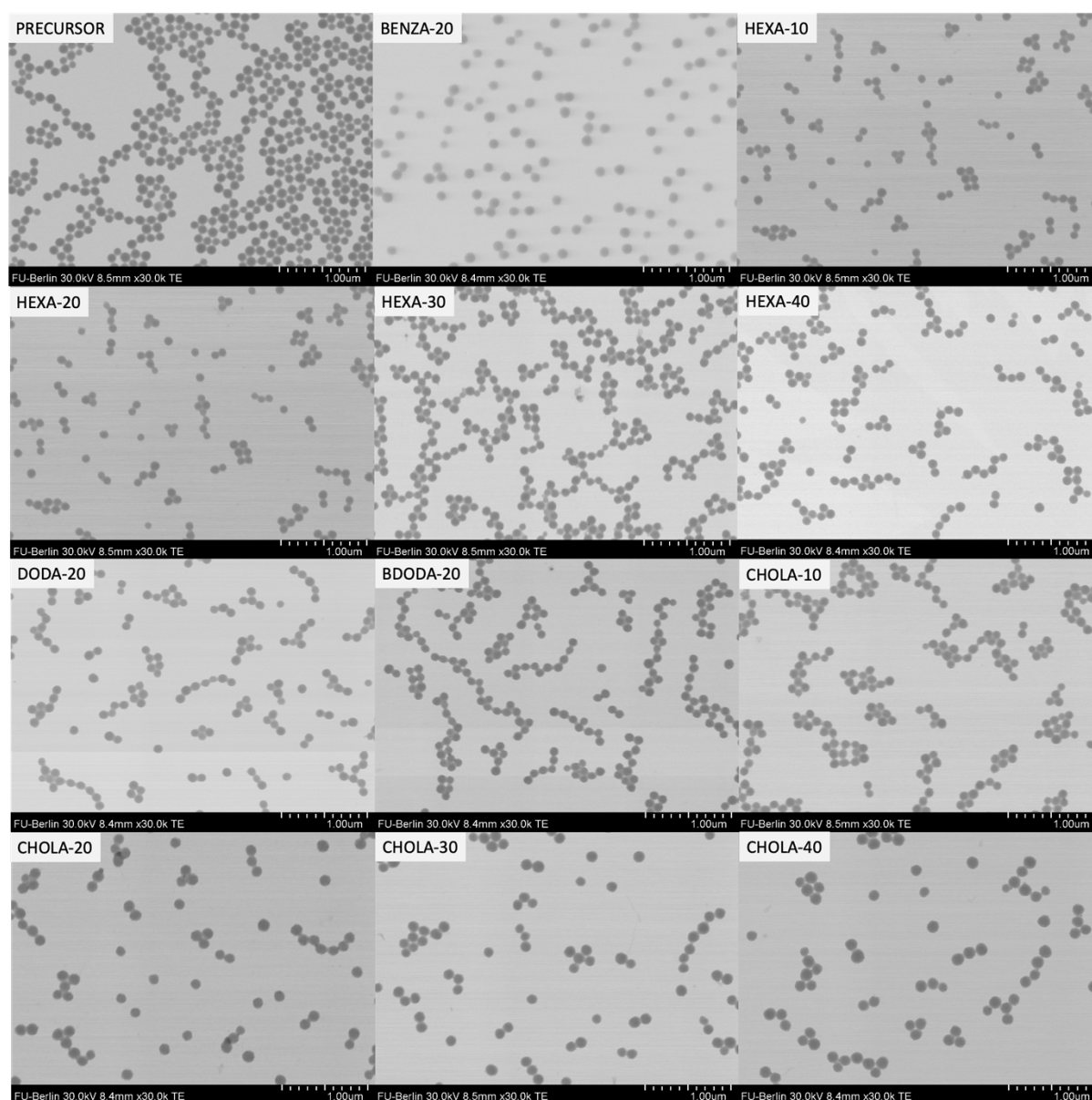


Figure S4. TEM images upon post-functionalization of the precursor particle resulted in morphologically and size uniform monodisperse particles. Images show the original reactive precursor particle, as particles functionalized with different hydrophobic groups (denoted as BENZA-20, HEXA-20, DODA-20, BDODA-20 and CHOLA-20) and particles functionalized with similar hydrophobic groups but different wt. % of hydrophobic groups (denoted as HEXA-10-40 and CHOLA-10-40).

1.1.3. Dynamic light scattering (DLS) of the NGs library

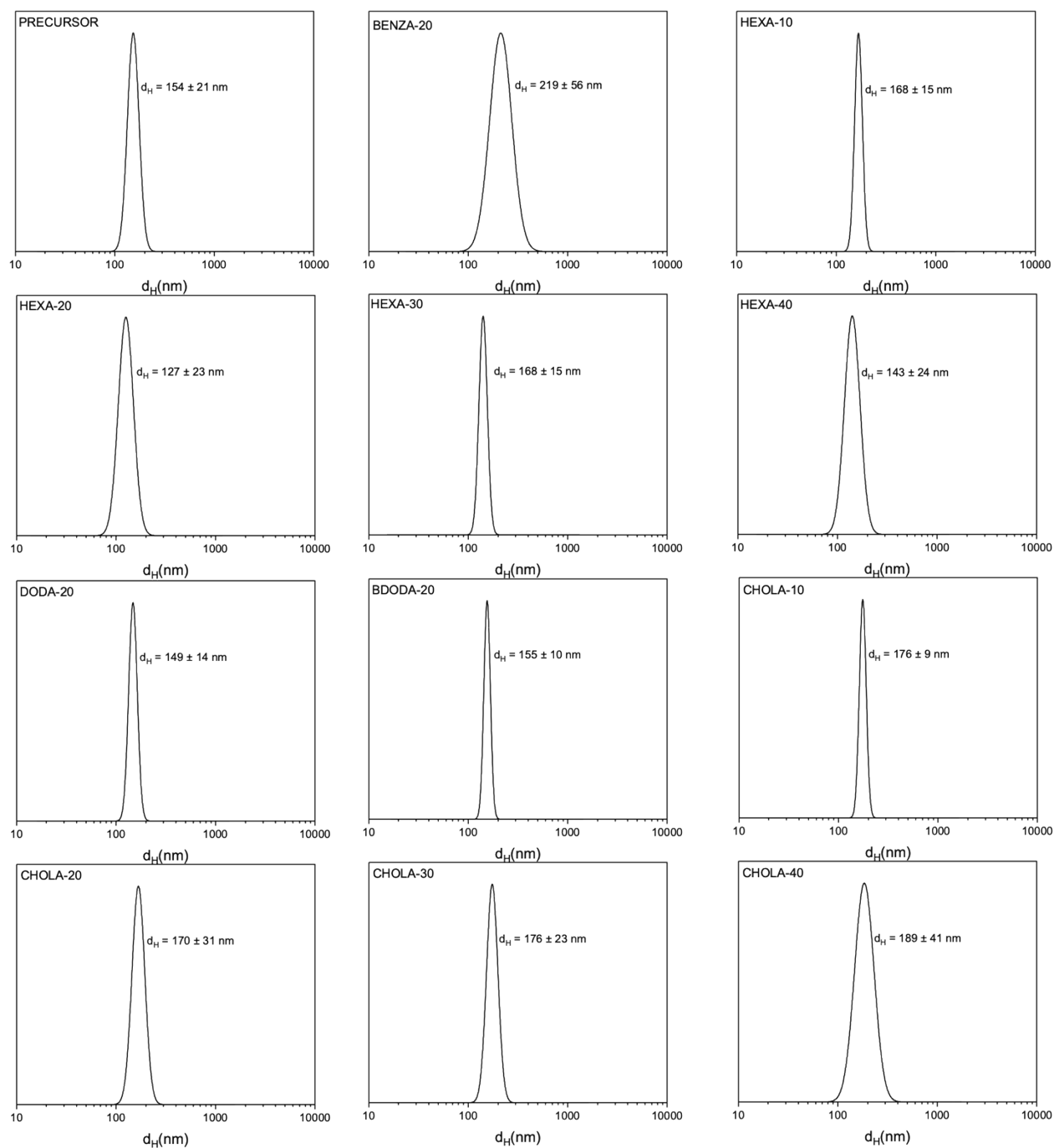


Figure S5. DLS data of the ANGs with different network amphiphilicity show well-defined colloidal particles with narrow size distribution.

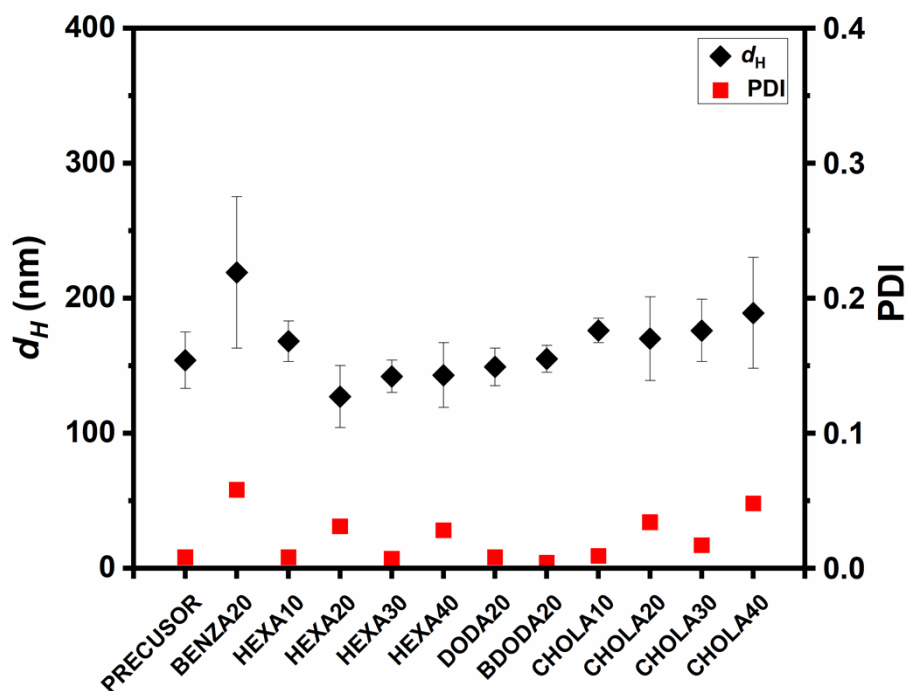


Figure S6. Functionalization of the reactive precursor particles gives access to well-defined ANGs with different hydrophobicity but similar colloidal features as size and particle size distribution (PDI). Almost all particles were measured in water, except to the precursor particle which was swollen in DMF.

1.2. Loading of amphiphilic nanogels with hydrophobic cargos

1.2.1. Calibration curves from UV/Vis spectrophotometry for the cargo library

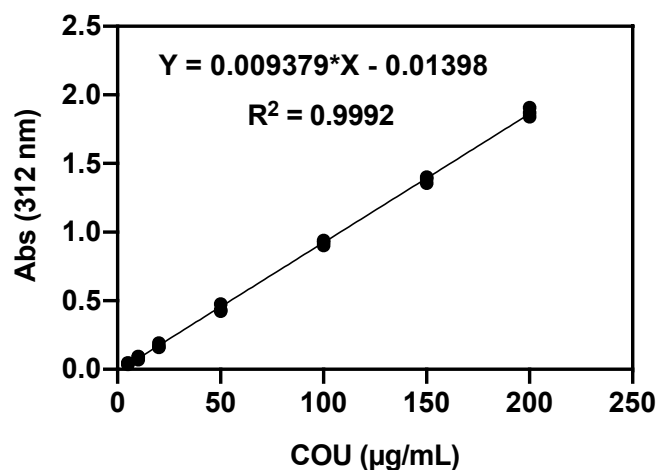


Figure S7. Calibration curve of coumarin in DMSO. Measured at 312 nm.

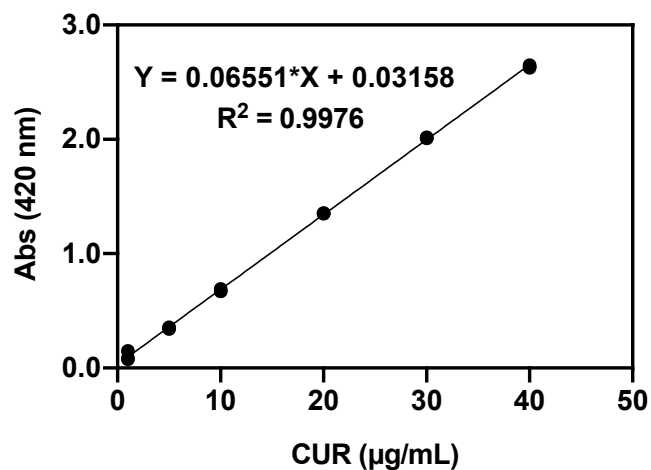


Figure S8. Calibration curve of curcumin in DMSO. Measured at 420 nm.

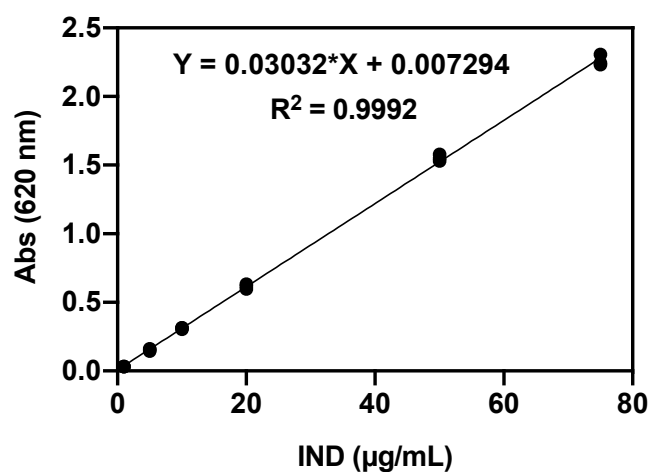


Figure S9. Calibration curve of indigo dye in DMSO. Measured at 620 nm.

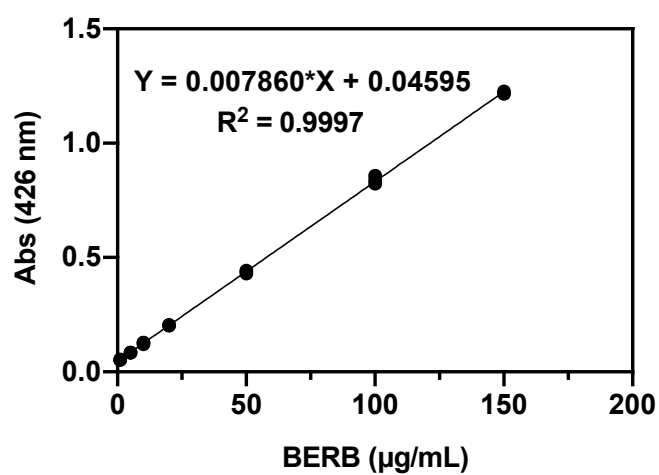


Figure S10. Calibration curve of berberine chloride dye in DMSO. Measured at 426 nm.

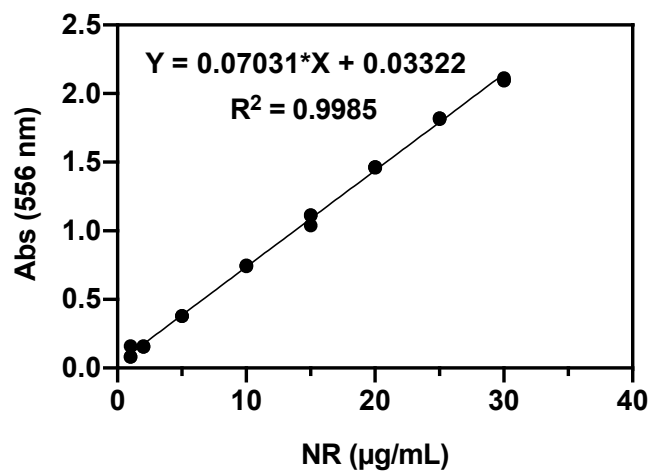


Figure S11. Calibration curve of Nile red dye in DMSO. Measured at 556 nm.

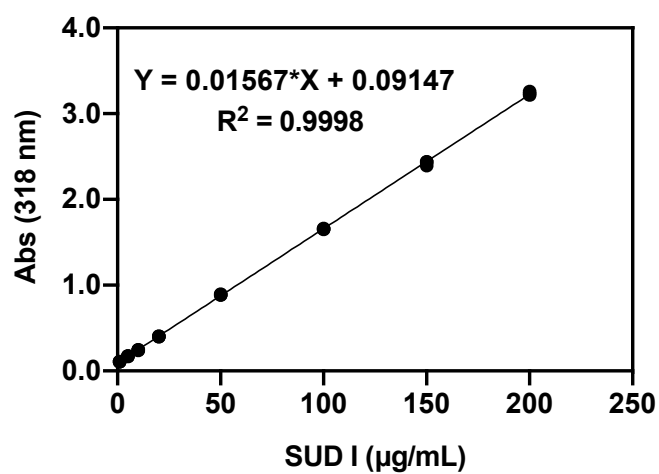


Figure S12. Calibration curve of Sudan I dye in DMSO. Measured at 318 nm.

1.2.2. Calibration curves from HPLC measurements for the cargo library

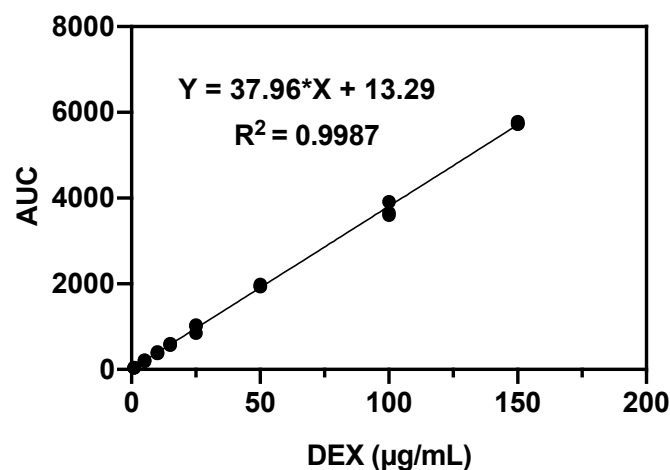


Figure S13. Calibration curve for HPLC determination of dexamethasone. Isocratic method with a mobile phase consisting of water/methanol 40:60. Flow rate was set at 1 mL/min and detection was carried out at 242 nm.¹

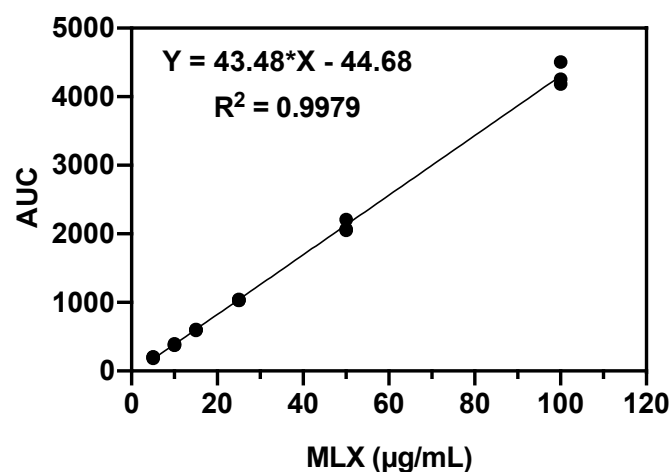


Figure S14. Calibration curve for HPLC determination of meloxicam. Isocratic method with a mobile phase consisting of acetonitrile/water 50:50 (pH adjusted to 3.0 with 0.1% sulfuric acid). Flow rate was set at 1.3 mL/min and detection was carried out at 362 nm.²

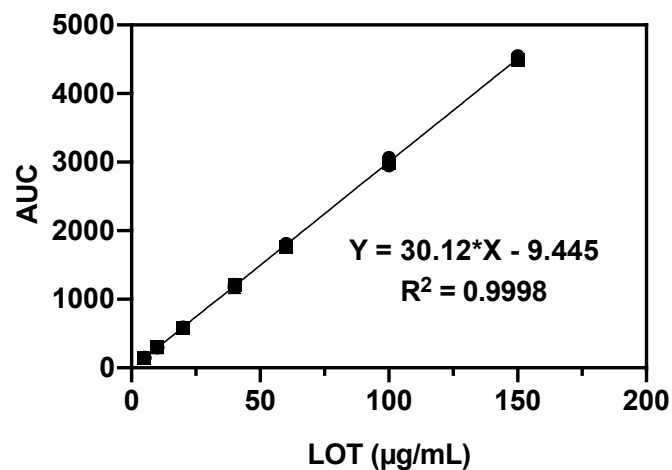


Figure S15. Calibration curve for HPLC determination of loteprednol etabonate. Isocratic method with a mobile phase consisting of water/acetonitrile/acetic acid 34.5:65:0.5. Flow rate was set at 1.1 mL/min and the drug was detected at 244 nm.³

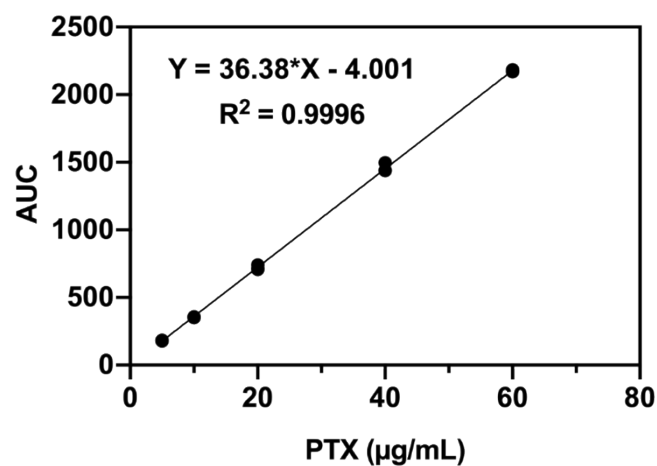


Figure S16. Calibration curve for HPLC determination of paclitaxel. Isocratic method with a mobile phase consisting of acetonitrile/water 55:45. Flow rate was set at 1.2 mg/mL and the drug was detected at 227 nm.⁴

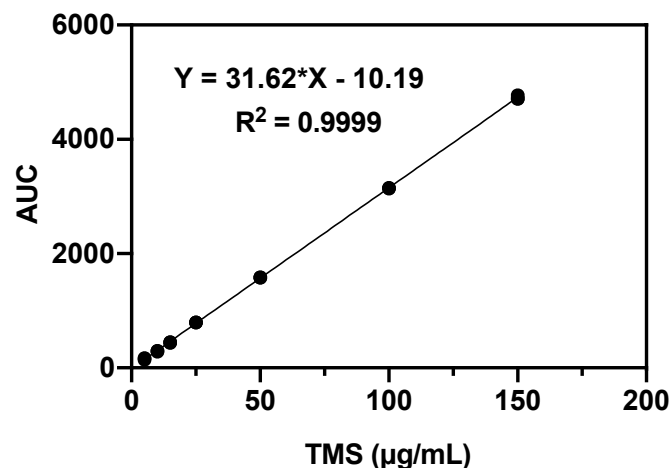


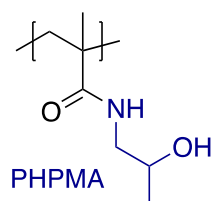
Figure S17. Calibration curve for telmisartan determination. Isocratic method with a mobile phase consisting of acetonitrile/aqueous 0.05M KH_2PO_4 pH 3.0 (adjusted with orthophosphoric acid). Flow rate was set at 1 mL/min, and telmisartan detection was carried out at 271 nm.⁵

2. Calculating solubility parameters for amphiphilic nanogels and cargos

2.1. Determination of Hansen solubility parameters (HSPs) for amphiphilic nanogels.

Group contributions for poly(2-Hydroxypropylmethacrylamine) (PHPMA)

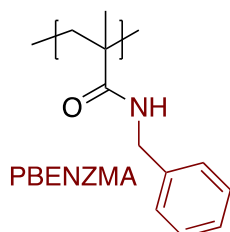
Table S1. Assignment of the different groups used to determine the molar volume V_m and cohesive energy (E_{coh}), also the partial and total solubility parameters δ_D , δ_P , δ_H and δ_T of PHPMA.



Group	Fedors Method	HVK Method
	for V_m and E_{coh}	for δ
Number of Groups		
-CH ₃	2	2
-CH ₂ -	2	2
>C<	1	1
-CONH-	1	
-CO-		1
-NH-		1
>CH-	1	1
-OH	1	1

Group contributions for poly(benzylmethacrylamine) (PBENZMA)

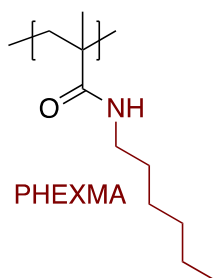
Table S2. Assignment of the different groups used to determine the molar volume V_m and cohesive energy (E_{coh}), also the partial and total solubility parameters δ_D , δ_P , δ_H and δ_T of PBENZMA.



Group	Fedors Method	HVK Method
	for V_m and E_{coh}	for δ
Number of Groups		
-CH ₃	3	3
-CH ₂ -	4	4
>C<	2	2
-CONH-	2	
-CO-		2
-NH-		2
>CH-	1	1
-OH	1	1
Phenyl	1	1

Group contributions for poly(hexylmethacrylamine) (PHEXMA)

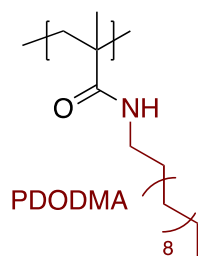
Table S3. Assignment of the different groups used to determine the molar volume V_m and cohesive energy (E_{coh}), also the partial and total solubility parameters δ_D , δ_P , δ_H and δ_T of PHEXMA.



Group	Fedors Method	HVK Method
	for V_m and E_{coh}	for δ
Number of Groups		
-CH ₃	4	4
-CH ₂ -	8	8
>C<	2	2
-CONH-	2	
-CO-		2
-NH-		2
>CH-	1	1
-OH	1	1

Group contributions for poly(dodecylmethacrylamine) (PDODMA)

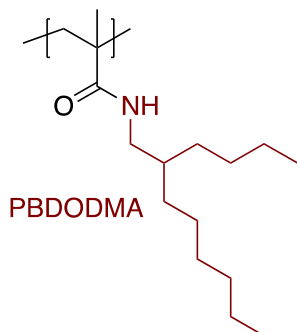
Table S4. Assignment of the different groups used to determine the molar volume V_m and cohesive energy (E_{coh}), also the partial and total solubility parameters δ_D , δ_P , δ_H and δ_T of PDODMA.



Group	Fedors Method for V_m and E_{coh}	HVK Method for δ
	Number of Groups	
-CH ₃	4	4
-CH ₂ -	14	14
>C<	2	2
-CONH-	2	
-CO-		2
-NH-		2
>CH-	1	1
-OH	1	1

Group contributions for poly(branched dodecylmethacrylamide) (PBDODMA)

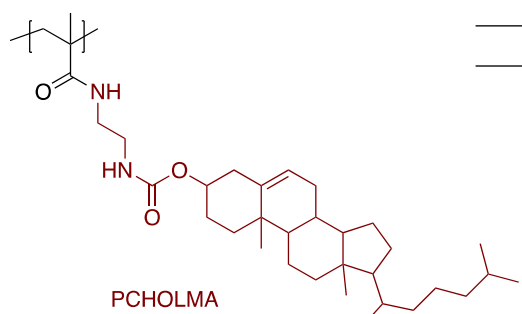
Table S5. Assignment of the different groups used to determine the molar volume V_m and cohesive energy (E_{coh}), also the partial and total solubility parameters δ_D , δ_P , δ_H and δ_T of PBDODMA.



Group	Fedors Method for V_m and E_{coh}	HVK Method for δ
	Number of Groups	
-CH ₃	5	5
-CH ₂ -	12	12
>C<	2	2
-CONH-	2	
-CO-		2
-NH-		2
>CH-	2	2
-OH	1	1

Group contributions for poly(Cholesteryl-based methacrylamide) (PCHOLMA)

Table S6. Assignment of the different groups used to determine the molar volume V_m and cohesive energy (E_{coh}), also the partial and total solubility parameters δ_D , δ_P , δ_H and δ_T of PCHOLMA.



Group	Fedors Method	HVK Method
	for V_m and E_{coh}	for δ
Number of Groups		
-CH ₃	8	8
-CH ₂ -	16	16
>C<	4	4
=CH-	1	1
>C=	1	1
-CONH-	2	
-CO-		2
-NH-		2
-NHCOO-	1	
-COO-		1
-NH-		1
>CH-	8	8
-OH	1	1
Ring (5 +)	3	
Ring (3-4)	1	
Ring		4

Hansen solubility parameters and molar volumes for all amphiphilic nanogels

Table S7. Calculated values of the partial (δ_D , δ_P and δ_H) and total solubility parameters (δ_T) for the ANG library.

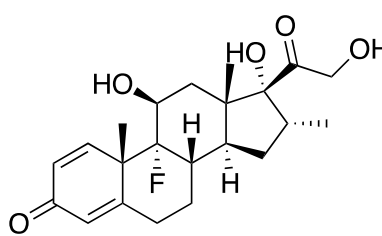
	HVK				YMB			
	δ_D	δ_P	δ_H	δ_T	δ_D	δ_P	δ_H	δ_T
HPA	9.6	9.6	16.0	20.8	17.0	17.0	14.9	18.6
BENZA-10	8.4	8.4	15.1	20.9	16.8	16.8	14.7	18.6
BENZA-20	7.4	7.4	14.2	21.0	16.4	16.4	14.2	18.8
BENZA-30	6.6	6.6	13.3	21.1	15.7	15.7	13.4	18.9
BENZA-40	5.9	5.9	12.5	21.2	14.9	14.9	12.5	19.1
HEXA-10	8.2	8.2	14.9	20.5	16.8	16.8	14.6	18.6
HEXA-20	7.0	7.0	13.9	20.1	16.2	16.2	14.0	18.7
HEXA-30	6.1	6.1	12.9	19.9	15.3	15.3	13.1	18.7
HEXA-40	5.4	5.4	11.9	19.6	14.2	14.2	12.0	18.8
DODA-10	7.5	7.5	14.3	20.1	16.4	16.4	14.3	18.6
DODA-20	6.0	6.0	12.8	19.6	15.3	15.3	13.2	18.6
DODA-30	4.9	4.9	11.5	19.2	13.8	13.8	11.7	18.5
DODA-40	4.1	4.1	10.4	18.9	12.4	12.4	10.4	18.5
BDODA-10	7.5	7.5	14.3	20.1	16.4	16.4	14.3	18.6
BDODA-20	6.0	6.0	12.8	19.6	15.2	15.2	13.1	18.6
BDODA-30	4.9	4.9	11.5	19.1	13.9	13.9	11.8	18.7
BDODA-40	4.1	4.1	10.4	18.8	12.5	12.5	10.4	18.7
CHOLA-10	6.3	6.3	13.3	19.9	15.5	15.5	13.5	18.6
CHOLA-20	4.5	4.5	11.5	19.3	13.3	13.3	11.5	18.6
CHOLA-30	3.4	3.4	10.2	19.0	11.6	11.6	9.9	18.6
CHOLA-40	2.8	2.8	9.2	18.8	10.2	10.2	8.6	18.7

All δ values are expressed in MPa^{1/2}

2.2. Determination of Hansen solubility parameters for drugs and dyes

Group contributions for Dexamethasone

Table S8. Assignment of the different groups used to determine the molar volume V_m and cohesive energy (E_{coh}), also the partial and total solubility parameters δ_D , δ_P , δ_H and δ_T of DEX.

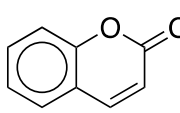


The chemical structure of Dexamethasone is shown, featuring a steroid nucleus with a ketone group at C3, a double bond between C4 and C5, a fluorine atom at C13, and hydroxyl groups at C11 and C14. A side chain at C17 includes a ketone group and a primary alcohol group.

Group	Fedors Method for V_m and E_{coh}	HVK Method for δ
	Number of Groups	
-CH ₃	3	3
-CH ₂ -	5	5
>CH-	4	4
>C<	4	4
=CH-	3	3
>C=	1	1
-F	1	1
-OH	3	3
>C=O (- CO-)	2	2
Ring (5 +)	4	
Ring		4

Group contributions for Coumarine

Table S9. Assignment of the different groups used to determine the molar volume V_m and cohesive energy (E_{coh}), also the partial and total solubility parameters δ_D , δ_P , δ_H and δ_T of COU.

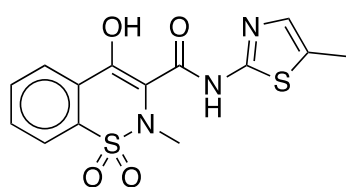


The chemical structure of Coumarine is shown, consisting of a benzene ring fused to a pyrone ring with a carbonyl group at the 2-position.

Group	Fedors Method for V_m and E_{coh}	HVK Method for δ
	Number of Groups	
Phenyl	1	1
-O-	1	
>C<	1	1
=CH-	2	2
>C=O (- CO-)	1	1
Ring (5 +)	1	
Ring		1

Group contributions for Meloxicam

Table S10. Assignment of the different groups used to determine the molar volume V_m and cohesive energy (E_{coh}), also the partial and total solubility parameters δ_D , δ_P , δ_H and δ_T of MLX.

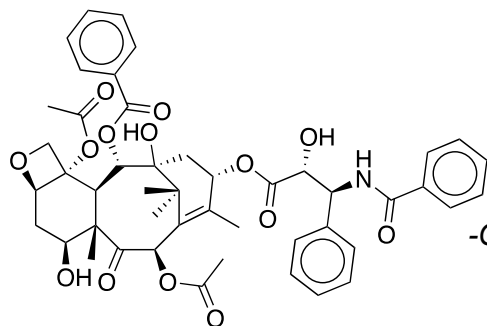


Group	Fedors Method	HVK Method
	for V_m and E_{coh}	for δ
Number of Groups		
Phenyl	1	1
-CH ₃	2	2
=CH-	1	1
>C=	4	4
-OH	1	1
-N<	1	1
>SO ₂ (>SO)	1	
-S- and -O-		1 and 2
-CONH-	1	
-CO- and -NH-		1 and 1
-S-	1	1
-N=	1	
-N< (-N=)		1
Ring (5 +)	2	
Ring		2

Group contributions for Paclitaxel

Table S11. Assignment of the different groups used to determine the molar volume V_m and cohesive energy (E_{coh}), also the partial and total solubility parameters δ_D , δ_P , δ_H and δ_T of PTX.

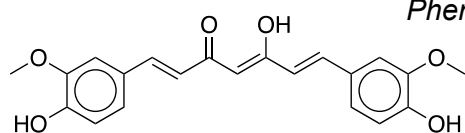
Group	Fedors Method	HVK Method
	for V_m and E_{coh}	for δ
Number of Groups		
-CH ₃	6	6
-CH ₂ -	3	3
>CH-	8	8
>C<	4	4
Phenyl	3	3
>C=	2	2
-COO-	4	4
-COO- (-COOR)		
-OH	3	3
>C=O (-CO-)	1	1
-CONH-	1	1
-CO- and -NH-		1 and 1
-O-	1	1
Ring (5+)	3	
Ring (3-4)	1	
Ring		4



Group contributions for Curcumin

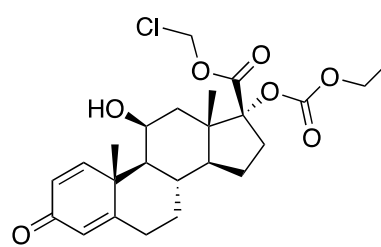
Table S12. Assignment of the different groups used to determine the molar volume V_m and cohesive energy (E_{coh}), also the partial and total solubility parameters δ_D , δ_P , δ_H and δ_T of CUR.

Group	Fedors Method	HVK Method
	for V_m and E_{coh}	for δ
Number of Groups		
-CH ₃	2	2
=CH-	5	5
>C=	1	1
Phenyl (trisubstituted)	2	2
-OH	3	3
>C=O (-CO-)	1	1
-O-	1	1
Plane of symmetry		1



Group contributions for Loteprednol

Table S13. Assignment of the different groups used to determine the molar volume V_m and cohesive energy (E_{coh}), also the partial and total solubility parameters δ_D , δ_P , δ_H and δ_T of LOT.

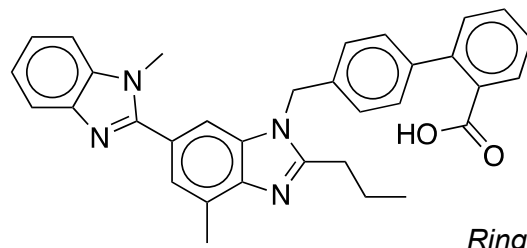


The chemical structure of Loteprednol is shown, featuring a complex steroid-like core with a chlorine atom, a hydroxyl group, and a carbonate ester group.

Group	Fedors Method	HVK Method
	for V_m and E_{coh}	for δ
	Number of Groups	
-CH ₃	3	3
-CH ₂ -	7	7
>CH-	4	4
>C<	3	3
=CH-	3	3
>C=	1	1
-CO ₃ - (carbonate)	1	
-COO- and -O-		1 and 1
-OH	1	1
>C=O (-CO-)	1	1
-CO ₂ -	1	1
-Cl	1	1
Ring (5 or more)	4	
Ring		4

Group contributions for Telmisartan

Table S14. Assignment of the different groups used to determine the molar volume V_m and cohesive energy (E_{coh}), also the partial and total solubility parameters δ_D , δ_P , δ_H and δ_T of TMS.

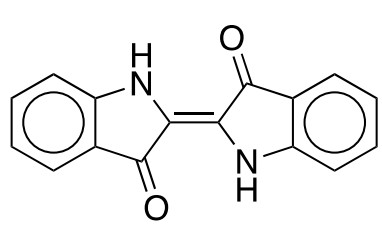


The chemical structure of Telmisartan is shown, featuring a central benzimidazole ring system with various substituents including a propyl group, a phenyl ring, and a carboxylic acid group.

Group	Fedors Method	HVK Method
	for V_m and E_{coh}	for δ
	Number of Groups	
Phenyl	2	4
Phenyl(o,m,p)	2	
-CH ₃	2	2
-CH ₂ -	3	3
>C=	2	2
>N-	2	2
-N=	2	
-N< (-N=)		2
-COOH	1	1
Ring (5 or more)	2	
Ring		2

Group contributions for Indigo

Table S15. Assignment of the different groups used to determine the molar volume V_m and cohesive energy (E_{coh}), also the partial and total solubility parameters δ_D , δ_P , δ_H and δ_T of IND.

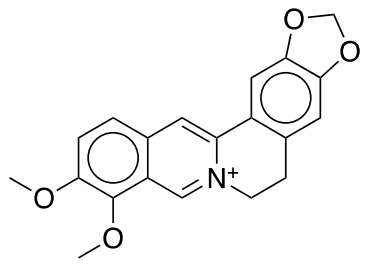


The chemical structure of Indigo shows two indole-like rings connected by a double bond at their 2-positions. Each ring has a carbonyl group at the 3-position and a hydrogen atom on the nitrogen at the 1-position.

Group	Fedors Method	HVK Method
	for V_m and E_{coh}	for δ
	Number of Groups	
Phenyl	2	2
-NH-	2	2
>C=	2	2
>C=O (-CO-)	2	2
Ring (5 +)	2	
Ring		2
Plane of symmetry		1

Group contributions for Berberine

Table S16. Assignment of the different groups used to determine the molar volume V_m and cohesive energy (E_{coh}), also the partial and total solubility parameters δ_D , δ_P , δ_H and δ_T of BER.

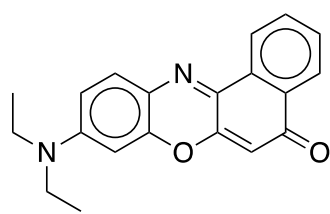


The chemical structure of Berberine is a complex polycyclic alkaloid. It features a central quaternary nitrogen atom (N+) within a piperidine ring. This ring is fused to a benzene ring, which is further fused to a quinoline-like system. The quinoline system has two methoxy groups (-OCH3) on one of its rings and a benzofuran-like ring system on the other.

Group	Fedors Method	HVK Method
	for V_m and E_{coh}	for δ
	Number of Groups	
-CH ₃	2	2
Phenyl	2	2
-CH ₂ -	3	3
=CH-	2	2
>C=	1	1
=N ⁺ (>N-)	1	1
-O-	4	4
Ring (5 or more)	3	
Ring		3

Group contributions for Nile Red

Table S17. Assignment of the different groups used to determine the molar volume V_m and cohesive energy (E_{coh}), also the partial and total solubility parameters δ_D , δ_P , δ_H and δ_T of NIL.

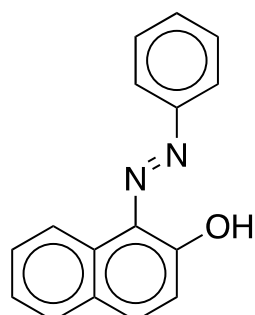


The chemical structure of Nile Red is shown, featuring a central benzoxazine ring system. It has a diethylamino group (-N(CH2CH3)2) attached to the benzene ring, a phenyl ring attached to the oxazine ring, and a coumarin-like structure fused to the oxazine ring, including a carbonyl group (=O).

Group	Fedors Method	HVK Method
	for V_m and E_{coh}	for δ
	Number of Groups	
-CH ₃	2	2
-CH ₂ -	2	2
Phenyl	2	2
>N-	1	1
-N=	1	
-N< (-N=)		1
=CH-	1	1
>C=	2	2
-O-	1	1
>C=O (-CO-)	1	1
Ring (5 or more)	2	
Ring		2

Group contributions for Sudan I

Table S18. Assignment of the different groups used to determine the molar volume V_m and cohesive energy (E_{coh}), also the partial and total solubility parameters δ_D , δ_P , δ_H and δ_T of SUD.



The chemical structure of Sudan I is shown, consisting of a naphthalene ring system. It has a hydroxyl group (-OH) at the 1-position and an azo group (-N=N-) at the 6-position, which is further connected to a phenyl ring.

Group	Fedors Method	HVK Method
	for V_m and E_{coh}	for δ
	Number of Groups	
Phenyl	3	3
-N=N-	1	
-N=N- (-N<)		2
-OH	1	1

Hansen solubility parameters for all drugs and dyes

Table. S19. Calculated values of the partial (δ_D , δ_P and δ_H) and total solubility parameters (δ_T) of various drugs.

	<i>HVK</i>				<i>YMB</i>			
	δ_D	δ_P	δ_H	δ_T	δ_D	δ_P	δ_H	δ_T
DEX	8.0	8.0	15.4	20.5	9.0	9.0	8.2	19.1
COU	8.0	8.0	6.7	21.3	12.5	12.5	6.7	20.0
MLX	8.0	8.0	13.6	26.2	17.5	17.5	13.3	21.0
PTX	5.3	5.3	13.2	21.3	8.1	8.1	3.7	20.0
CUR	4.2	4.2	10.2	22.8	7.5	7.5	12.9	20.2
LOT	4.5	4.5	10.9	17.2	7.3	7.3	20.4	18.6
TMS	8.7	8.7	9.0	21.8	3.3	3.3	2.8	21.4
IND	4.2	4.2	7.3	22.1	17.4	17.4	10.0	21.1
BER	5.4	5.4	7.1	17.9	4.6	4.6	6.4	20.5
NIL	6.4	6.4	7.2	18.8	8.0	8.0	5.1	19.5
SUD	7.6	7.6	11.6	20.3	3.9	3.9	7.8	20.7

δ values are expressed in MPa^{1/2}

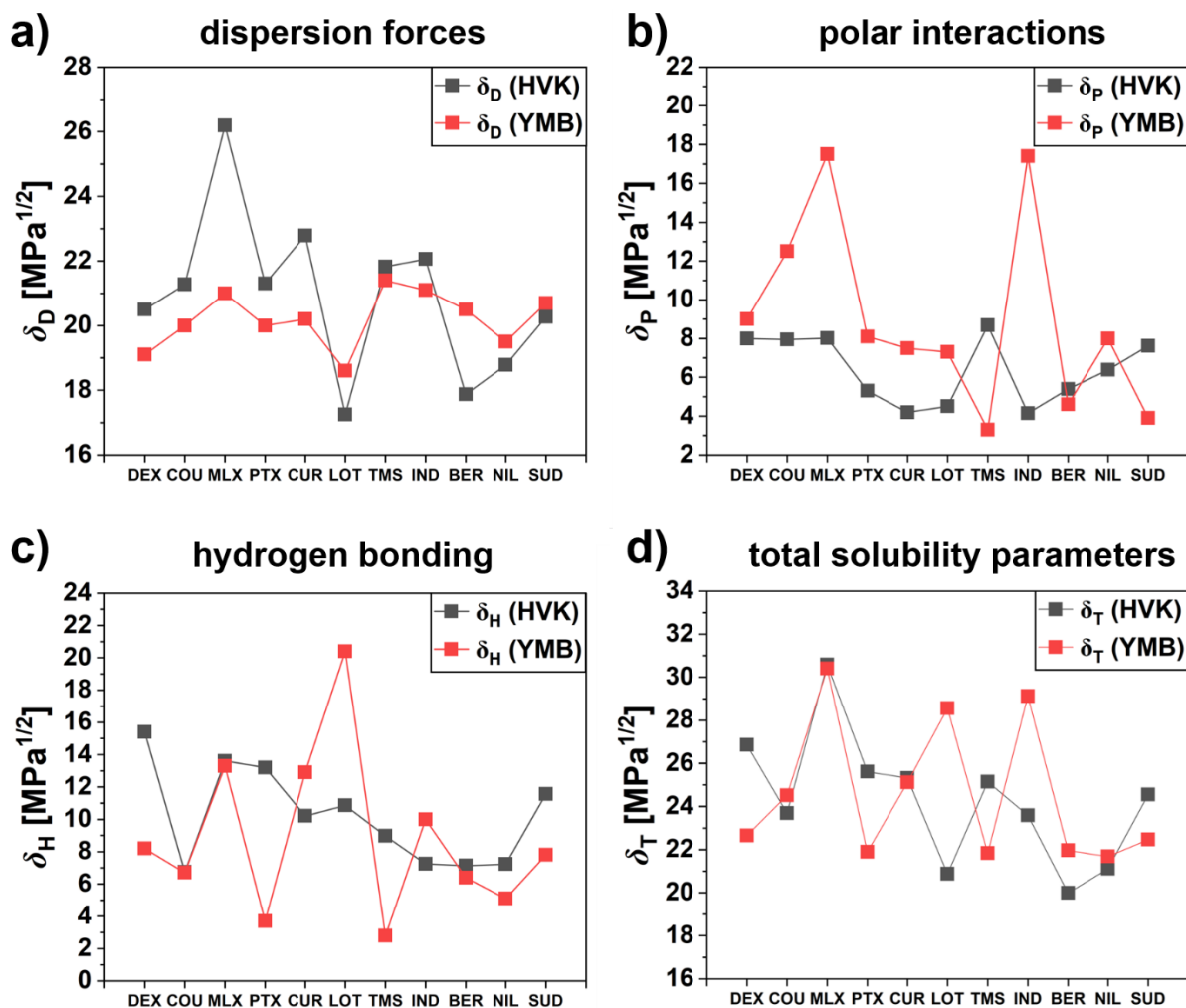


Figure S18. Hansen solubility parameters from the HVK and the YMB method showed similar predictions only for a subset of drugs. This behavior is observed for the individual solubility parameters that represent the contributions of (a) dispersion forces, (b) polar interactions, and (c) hydrogen bonding and their combination to the total solubility parameter (d). The level of agreement between the two methods depends on the molecular structure of the drugs- such as their polarity, hydrogen-bonding capacity and functional group composition.

2.3. Calculation of Hildebrand solubility parameters

The Hildebrand solubility parameter (δ) is defined as square root of the cohesive molecular energy density (CED).⁶

$$\delta = \sqrt{CED} = \sqrt{\frac{E_{coh}}{V_m}} = \sqrt{\frac{\Delta H_{vap} - RT}{V_m}} \quad (1)$$

The CED is the cohesive energy (E_{coh}) per unit of molar volume (V_m), that is required to expel molecules from its adjacent neighbour. The cohesive energy can be derived from heat of vaporization energy (ΔH_{vap}) at a given temperature (T). In the present work, Hildebrand SPs and molar volume (V_m) were calculated for whole amphiphilic nanogel and drug library using indirect group contribution method (GCM) given by Fedors.⁶⁻⁸ According to Fedors' method, the molar volume (V_m) and cohesion energy (E_{coh}) is defined as sum of each structural groups specific volume or energy, multiplied by the number (n_i) of times the structural group i occurs in the molecule:

$$V_m = \sum n_i V_i \quad (2)$$

$$E_{coh} = \sum n_i E_i \quad (3)$$

These values are calculated for the ANGs' repeat units and cargoes as shown in Table S20 and Table S21.

2.3.1. Cohesive energies, molar volumes and Hildebrand solubility parameters for amphiphilic nanogels

Table S20. Calculated values of the molar volume V_m and cohesive energy (E_{coh}) of NGs repeating unit.

	Fedors	
	V_m¹⁾	E_{coh}²⁾
HPA	98.5	87490
PBENZMA	127.4	81490
PHEXMA	153.9	74020
PDODAMA	250.5	103660
PBDODMA	250.8	101920
PCHOLMA	478.8	200610

¹⁾ V_m values are expressed in $\text{cm}^3\text{mol}^{-1}$;

²⁾ E_{coh} values are expressed in $\text{J}^{-1}\text{mol}^{-1}$

2.3.2. Cohesive energies and molar volumes for drugs and dyes

Table S21. Calculated values of the molar volume V_m and cohesive energy (E_{coh}) for all drugs and dyes.

	<i>Fedors</i>	
	$V_m^{1)}$	$E_{\text{coh}}^{2)}$
DEX	269	207840
COU	110	63800
MLX	189	197150
PTX	560	402740
CUR	240	209280
LOT	334	182580
TMS	372	2346000
IND	194	126080
BER	334	125010
NIL	287	130530
SUD	224	129810

3. PART A – Numerical parameters for ANG-cargo interactions: Combining CHOLA-20 particles with library of different cargos

3.1. Calculation of Flory-Huggins interaction parameters and optimization of α -values

Flory-Huggins interaction Parameters for CHOLA20-cargo

Flory-Huggins interaction parameters between cargo and ANGs ($\chi_{\text{ca,ANG}}$) were calculated from the individual Hansen solubility parameters and V_m values (Tables S7 and S19) according to equation 4:

$$\chi_{\text{ca,ANG}} = \alpha \frac{V_{m,\text{ca}}}{RT} ((\delta_{D,\text{ca}} - \delta_{D,\text{ANG}})^2 + 0.25(\delta_{P,\text{ca}} - \delta_{P,\text{ANG}})^2 + 0.25(\delta_{H,\text{ca}} - \delta_{H,\text{ANG}})^2) \quad (4)$$

Calculation of the individual solubility parameters is described in the experimental section of the main article.

Table S22. Determination of compatibility between various drugs and CHOLA-20 nanogel. method and Estimated values of the Flory-Huggins interaction (χ) parameters calculated by HVK and YMB. Calculations are based on varying α and include data for χ : according to **Hansen original framework with $\alpha = 1$** and **Lindvig's method with $\alpha = 0.6$** for all cargo, as well as for **α -adjusted calculations $\alpha = 1$** for cargos with dominant dispersion forces (**Group 1**), **$\alpha = 0.6$** for cargos with dominant polar interactions (**Group 2**) and **$\alpha = 0.3$** for cargos with dominant H-bonding interactions (**Group 3**) according to our previous work. Correlation of these χ values with experimentally-determined LCs from Figure 1 gives the **corrected Spearman correlation coefficients (ρ)**.

CHOLA-20 + cargo	χ (HVK)	χ (YMB)	χ (HVK)	χ (YMB)	χ (HVK)			χ (YMB)		
	$\alpha =$		$\alpha =$		$\alpha =$			$\alpha =$		
	1		0.6		1	0.6	0.3	1	0.6	0.3
PTX	1.07	5.42	0.64	3.25	1.07	-	-	5.42	-	-
TMS	1.83	2.60	1.10	1.56	1.83	-	-	2.60	Group 1	-
BER	0.96	2.82	0.58	1.69	0.96	Group 2	-	2.82		-
NIL	0.67	1.91	0.40	1.15	0.67		-	1.91		-
SUD	0.30	0.98	0.18	0.59	0.30		-	0.98	-	
COU	0.55	0.35	0.33	0.21	0.55	-	-	-	0.21	Group 3
MLX	3.90	0.84	2.34	0.50	-	-	1.17	-	0.50	
IND	0.94	2.93	0.56	1.76	-	Group 3	0.28	-	1.76	
DEX	0.90	0.82	0.54	0.49	-		0.27	-	-	0.25
CUR	1.20	3.75	0.72	2.25	-		0.36	-	-	1.13
LOT	0.61	2.87	0.37	1.72	-	-	0.18	-	-	0.86
ρ	-0.28	-0.83	-0.28	-0.85	-0.25			-0.87		

all values for χ expressed in MPa^{1/2}

a) HVK - method



b) YMB - method

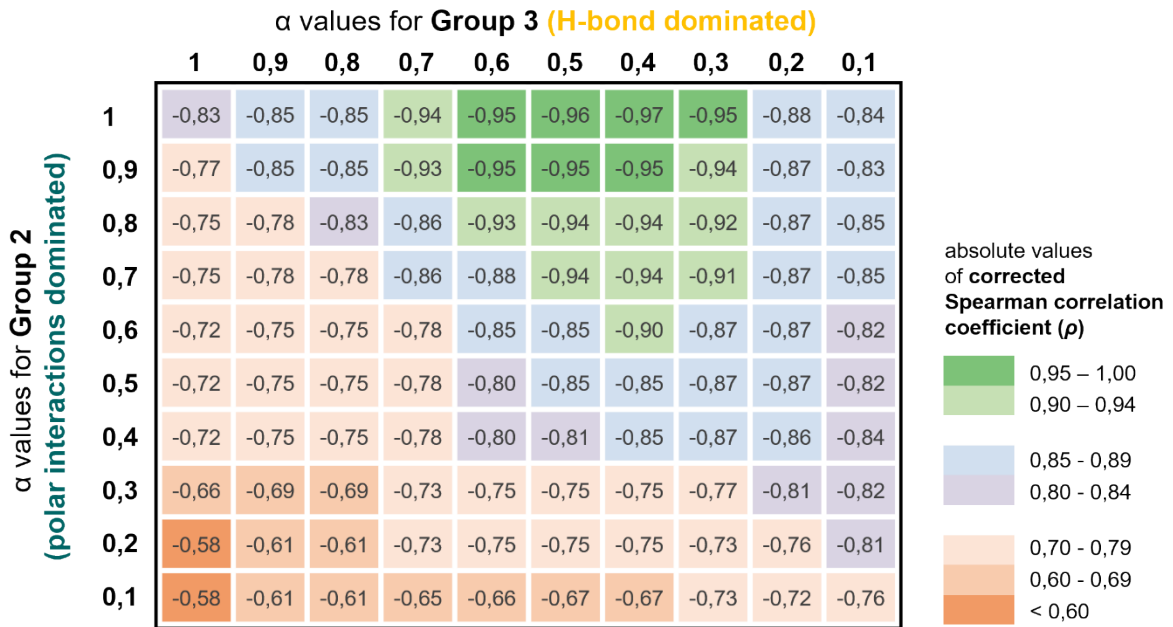


Figure S19. Optimization of α values for cargos of Group 2 and Group 3 by analyzing the correlation between experimental LC and α -adjusted χ . Corrected Spearman correlation coefficients (ρ) between LC and χ serve as quantitative measure for correlation of data that includes χ from (a) HVK method and (b) YMB method.

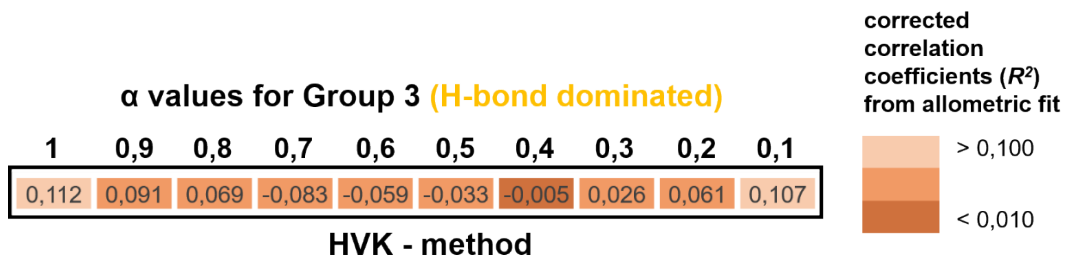


Figure S20. Optimization of α values for cargos of Group 3 by analyzing the correlation between experimental LC and α -adjusted χ (from HVK). Corrected correlation coefficients (R^2) of allometric fits between LC and χ serve as quantitative measure for correlation and show no pronounced correlation..

3.2. Correlating Flory-Huggins parameters from HVK method with experimental loading contents

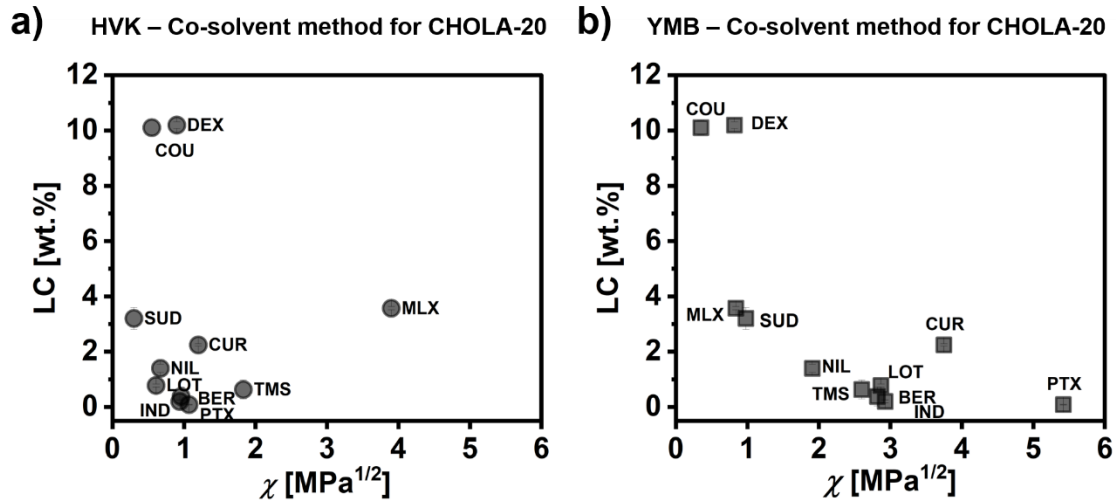


Figure S21. Correlating experimental loading contents with the non-adjusted Flory-Huggins interaction parameters between CHOLA-20 ANGs and cargoes (i.e., Hansen framework $\alpha = 1$) does not show a clear trend for (a) the HVK method or (b) the YMB method.

3.3. Calculation of Hildebrand solubility parameters

The differences in Hildebrand solubility parameters between cargo and ANGs were calculated from the individual values for cargo and ANG (Table S23) according to equation 5:

$$|\Delta\delta| = \delta_{ca} - \delta_{ANG} \quad (6)$$

For the ANGs, the calculation of δ needs to consider the random copolymer structure of the network. Here, the copolymer chains contain a mixture of two different monomers, e.g., poly(2-hydroxypropylmethacrylamide-*co*-hexylmethacrylamide) P(HPMA-*co*-HEXMA). Thus, the molar volume and the cohesive energy contributions need to be calculated for each type of repeating unit, i.e., $V_{m,HPMA}$; $V_{m,HEXMA}$, $E_{coh,HPMA}$, and $E_{coh,HEXMA}$. Furthermore, the molar fractions of the different monomers need to be considered. Thus, for P(HPMA-*co*-HEXMA), the molar fraction of HPMA in the copolymer is represented by f_{HPMA} and the molar fraction of HEXMA is represented by f_{HEXMA} . Similarly, the molar volume of HPMA is denoted as $V_{m,HPMA}$, while the molar volume of HEXMA is denoted as $V_{m,HEXMA}$, respectively. The overall number of repeating units in each chain does not influence the solubility parameters and can be neglected. Taking these considerations into account, the Hildebrand solubility parameters were calculated:

$$\delta = \sqrt{\frac{f_{HPMA}E_{coh,HPMA} + f_{HEXMA}E_{coh,HEXMA}}{f_{HPMA}V_{m,HPMA} + f_{HEXMA}V_{m,HEXMA}}} \quad (7)$$

Table S23. Calculated values of the Hildebrand solubility parameters δ for various drugs and CHOLA-20 nanogel.

	δ [MPa ^{1/2}]	$ \Delta\delta $ [MPa ^{1/2}]
CHOLA-20	25.1	-
DEX	27.8	2.7
COU	24.1	1.0
MLX	32.3	7.2
PTX	26.8	1.7
CUR	29.5	4.4
LOT	23.3	1.8
TMS	24.3	0.8
IND	25.5	0.4
BER	19.1	6.0
NIL	21.8	3.3
SUD	24.1	1.0

3.4. Correlating Hildebrand solubility parameters with experimental loading contents

Hildebrand SPs were calculated for the combination of CHOLA-20 and the cargo library. In agreement with the principle “like dissolves like”, a small value for $|\Delta\delta|$ between nanogel carrier and cargo suggests a stronger interaction and thus a higher drug loading capability. However, as shown in Figure S22, the relationship between calculated $|\Delta\delta|$ and experimental LC does not show a clear trend.

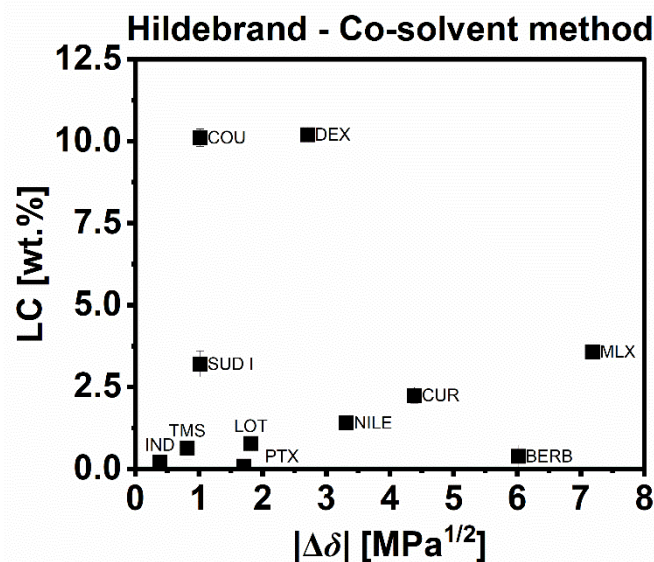


Figure S22. Correlating experimental loading contents with the difference in Hildebrand solubility parameters $|\Delta\delta|$ between CHOLA-20 ANGs and cargos does not show a clear trend.

3.5. Calculation of the distance of Hansen solubility parameters R_a

The Distance of the Hansen solubility parameters R_a were calculated⁶ from the individual HSPs in Tables S8 and S20 according to equation 5:

$$R_a^2 = 4(\delta_{D,ca} - \delta_{D,ANG})^2 + (\delta_{P,ca} - \delta_{P,ANG})^2 + (\delta_{H,ca} - \delta_{H,ANG})^2 \quad (5)$$

Calculation of the individual solubility parameters is described in the experimental section of the main article.

Table S24. Determination of compatibility between various drugs and CHOLA-20 nanogel calculated by HVK and YMB method and estimated values of the distance R_a .

	R_a (HVK)	R_a (YMB)
DEX	5.74	5.51
COU	7.06	5.61
MLX	14.31	6.63
PTX	4.35	9.78
CUR	7.03	6.77
LOT	4.24	10.73
TMS	6.99	14.39
IND	6.92	6.64
BER	5.35	10.78
NIL	4.82	8.50
SUD	3.66	10.94

3.6. Correlating R_a with experimental loading contents

Conventionally, the distance between the total HSPs of cargo and ANG in the 3-dimensional Hansen space is often used to estimate interactions. Here, the solubility of a cargo molecule in a nanogel network can be estimated as the distance R_a (see ESI section 3.1., Table S22). Applying this approach for the combination of CHOLA-20 nanogels with different cargos gave no clear correlation between LC and R_a (Figure S23). This result was independent from the used underlying group contribution method, i.e. HVK or YMB.

We attribute this to the fact that the Hansen distance R_a only provides qualitative insight into relative solubility. This is because it treats all interaction energies equally, ignores molar volumes, and cannot capture variations in energy contributions arising from entropic constraints.

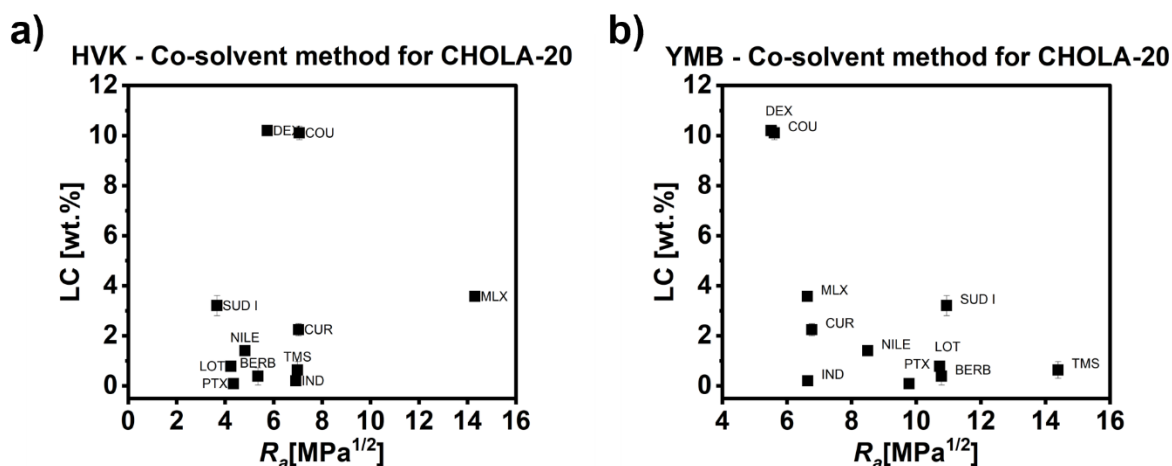


Figure S23. Combination of cargo library with CHOLA-20 ANGs - Correlation of experimental loading contents (LC) with calculated by HVK (a) and YMB (b) method: LC does not correlate well with R_a values.

4. PART B - Influence of the type of hydrophobic groups on the correlation between numerical parameters and cargo loading contents

4.1. Calculation of Flory-Huggins parameters and R_a values for the combination of amphiphilic nanogels with coumarin, curcumin and Nile red

Table S25. Determination of compatibility between **coumarin (COU)** and the ANGs with different network amphiphilicity. Estimated values of distance R_a and the Flory-Huggins interaction (χ) parameter (corrected by value α) were calculated by HVK and YMB method. Cargo was loaded by co-solvent method.

	χ	χ	R_a	R_a	LC	
	(HVK)	(YMB)	(HVK)	(YMB)	experimental Mean	SD
	$\alpha = 1$	$\alpha = 0.7$				
BENZA-20	0.63	0.60	7.52	8.79	5.75	1.13
HEXA-20	0.63	0.57	7.54	8.59	6.94	0.26
DODA-20	0.57	0.45	7.15	7.61	8.10	0.91
BDODA-20	0.58	0.44	7.22	7.49	8.73	0.31
CHOLA-20	0.55	0.24	7.06	5.61	10.21	0.33

χ and R_a values are expressed in MPa^{1/2}; LC values are expressed in %

Table S26. Determination of compatibility between **curcumin (CUR)** and the ANGs with different network amphiphilicity. Estimated values of distance R_a and the Flory-Huggins interaction (χ) parameter (corrected by value α) were calculated by HVK and YMB method. with. Cargo was loaded by co-solvent method.

	χ (HVK)	χ (YMB)	R_a (HVK)	R_a (YMB)	LC <i>experimental</i>	
	$\alpha = 1$	$\alpha = 0.3$			Mean	SD
BENZA-20	0.93	1.66	6.21	9.42	1.00	0.09
HEXA-20	1.20	1.64	7.03	9.27	1.36	0.04
DODA-20	1.20	1.47	7.04	8.44	1.47	0.10
BDODA-20	1.24	1.45	7.16	8.34	1.70	0.10
CHOLA-20	1.20	1.12	7.03	6.77	2.24	0.04

χ and R_a values are expressed in $\text{MPa}^{1/2}$; LC values are expressed in %

Table S27. Determination of compatibility between **Nile red (NIL)** and the ANGs with different network amphiphilicity. Estimated values of distance R_a and the Flory-Huggins interaction (χ) parameter (corrected by value α) were calculated by HVK and YMB method. with. Cargo was loaded by co-solvent method.

	χ (HVK)	χ (YMB)	R_a (HVK)	R_a (YMB)	LC <i>experimental</i>	
	$\alpha = 1$	$\alpha = 1$			Mean	SD
BENZA-20	2.04	4.31	8.39	12.46	0.88	0.03
HEXA-20	1.51	4.11	7.22	12.21	1.02	0.06
DODA-20	0.99	3.33	5.84	11.05	1.14	0.01
BDODA-20	0.97	3.25	5.80	10.91	1.13	0.02
CHOLA-20	0.67	1.91	4.82	8.50	1.4	0.15

χ and R_a values are expressed in $\text{MPa}^{1/2}$; LC values are expressed in %

4.2. Influence of hydrophobic structure on the correlation between Flory-Huggins interaction parameters (calculated by HVK method) and cargo LC

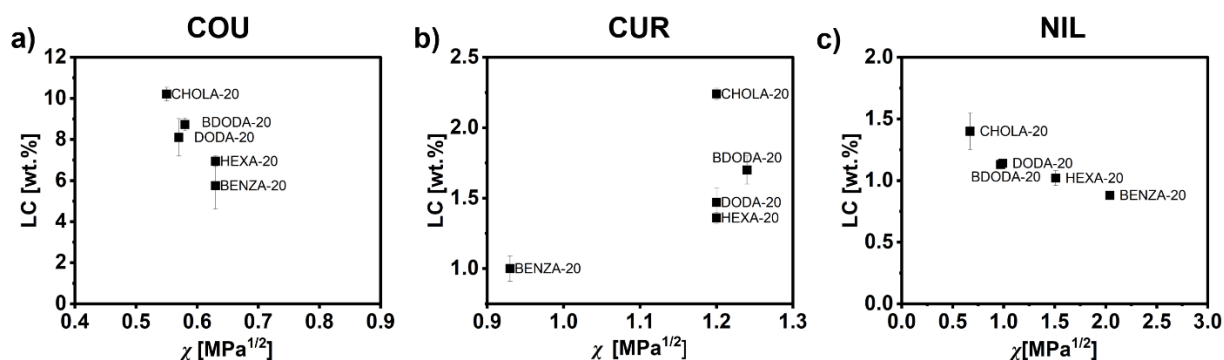


Figure S24. χ values of the NGs library with coumarin (a), curcumin (b) and Nile red (c) calculated by HVK method in correlation with LC determined by co-solvent loading method.

4.3. Influence of hydrophobic structure on the correlation between R_a and cargo LC (comparison of HVK and YMB method)

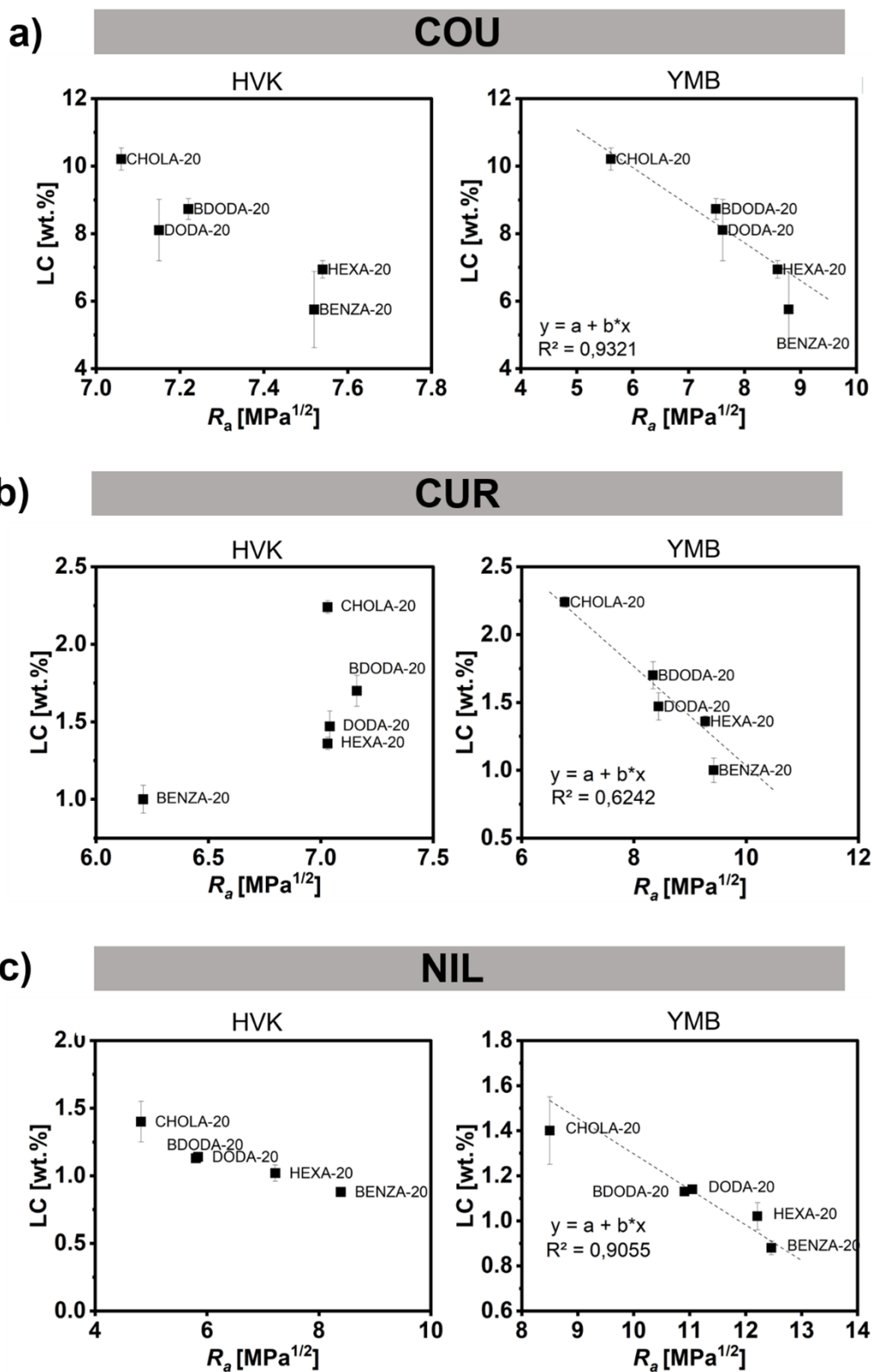


Figure S25. R_a values of the NGs library with coumarin (a), curcumin (b) and Nile red (c) calculated by HVK and YMB method in correlation with LC determined by co-solvent loading method.

5. PART C - Influence of hydrophobic content on the correlation between numerical parameters and cargo LC

5.1. Calculation of Flory-Huggins parameters and R_a values for the combination of amphiphilic nanogels with coumarin, curcumin and Nile red

Table S28. Determination of compatibility between coumarin (COU) and the ANGs with different network amphiphilicity. Estimated values of distance R_a and the Flory-Huggins interaction (χ) parameter (corrected by value α) were calculated by HVK and YMB method. with. Cargo was loaded by co-solvent method.

	χ (HVK)	χ (YMB)	R_a (HVK)	R_a (YMB)	LC	
	$\alpha = 1$	$\alpha = 0.7$			experimental Mean	SD
HEXA-10	0.77	0.69	8.32	9.42	5.57	0.36
HEXA-20	0.63	0.57	7.54	8.59	6.94	0.26
HEXA-30	0.54	0.43	7.00	7.45	8.91	0.71
HEXA-40	0.49	0.29	6.66	6.06	10.03	0.36
CHOLA-10	0.59	0.49	7.32	7.94	8.71	0.59
CHOLA-20	0.55	0.24	7.06	5.61	10.21	0.33
CHOLA-30	0.59	0.15	7.30	4.35	13.41	0.78
CHOLA-40	0.64	0.12	7.62	3.96	14.74	1.21

χ and R_a values are expressed in MPa^{1/2}; LC values are expressed in %

Table S29. Determination of compatibility between curcumin (CUR) and the ANGs with different network amphiphilicity. Estimated values of distance R_a and the Flory-Huggins interaction (χ) parameter (corrected by value α) were calculated by HVK and YMB method. with. Cargo was loaded by co-solvent method.

	χ (HVK)	χ (YMB)	R_a (HVK)	R_a (YMB)	LC	
	$\alpha = 1$	$\alpha = 0.3$			experimental Mean	SD
HEXA-10	1.44	1.80	7.72	9.98	0.99	0.20
HEXA-20	1.20	1.64	7.03	9.27	1.36	0.04
HEXA-30	1.09	1.44	6.71	8.36	1.94	0.13
HEXA-40	1.08	1.21	6.69	7.32	2.21	0.47
CHOLA-10	1.16	1.52	6.92	8.64	1.37	0.36
CHOLA-20	1.20	1.12	7.03	6.77	2.24	0.04
CHOLA-30	1.41	0.91	7.63	6.00	2.43	0.18
CHOLA-40	1.65	0.77	8.25	5.90	2.82	0.04

χ and R_a values are expressed in MPa^{1/2}; LC values are expressed in %

Table S30. Determination of compatibility between **Nile red (NIL)** and the ANGs with different network amphiphilicity. Estimated values of distance R_a and the Flory-Huggins interaction (χ) parameter (corrected by value α) were calculated by HVK and YMB method. with. Cargo was loaded by co-solvent method.

	χ	χ	R_a	R_a	LC	
	(HVK)	(YMB)	(HVK)	(YMB)	experimental	SD
	$\alpha = 1$	$\alpha = 1$			Mean	SD
HEXA-10	2.12	4.71	8.57	13.07	0.83	0.02
HEXA-20	1.51	4.11	7.22	12.21	1.02	0.06
HEXA-30	1.06	3.30	6.06	10.95	1.13	0.02
HEXA-40	0.74	2.43	5.06	9.38	1.24	0.05
CHOLA-10	1.20	3.54	6.44	11.40	1.08	0.04
CHOLA-20	0.67	1.91	4.82	8.50	1.4	0.15
CHOLA-30	0.52	1.00	4.23	6.26	1.80	0.07
CHOLA-40	0.49	0.48	4.12	4.43	2.24	0.17

χ and R_a values are expressed in $\text{MPa}^{1/2}$; LC values are expressed in %

5.2. Influence of hydrophobic content on the correlation between Flory-Huggins interaction parameters (calculated by HVK method) and cargo LC

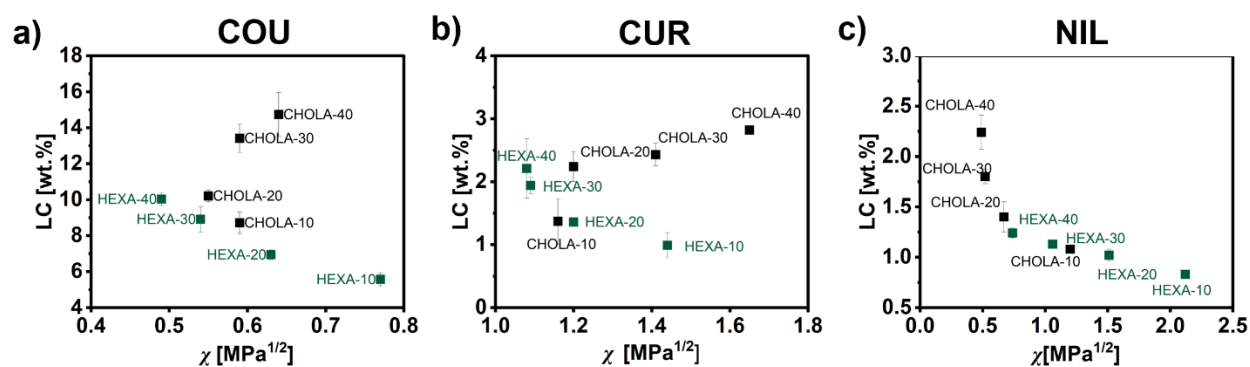
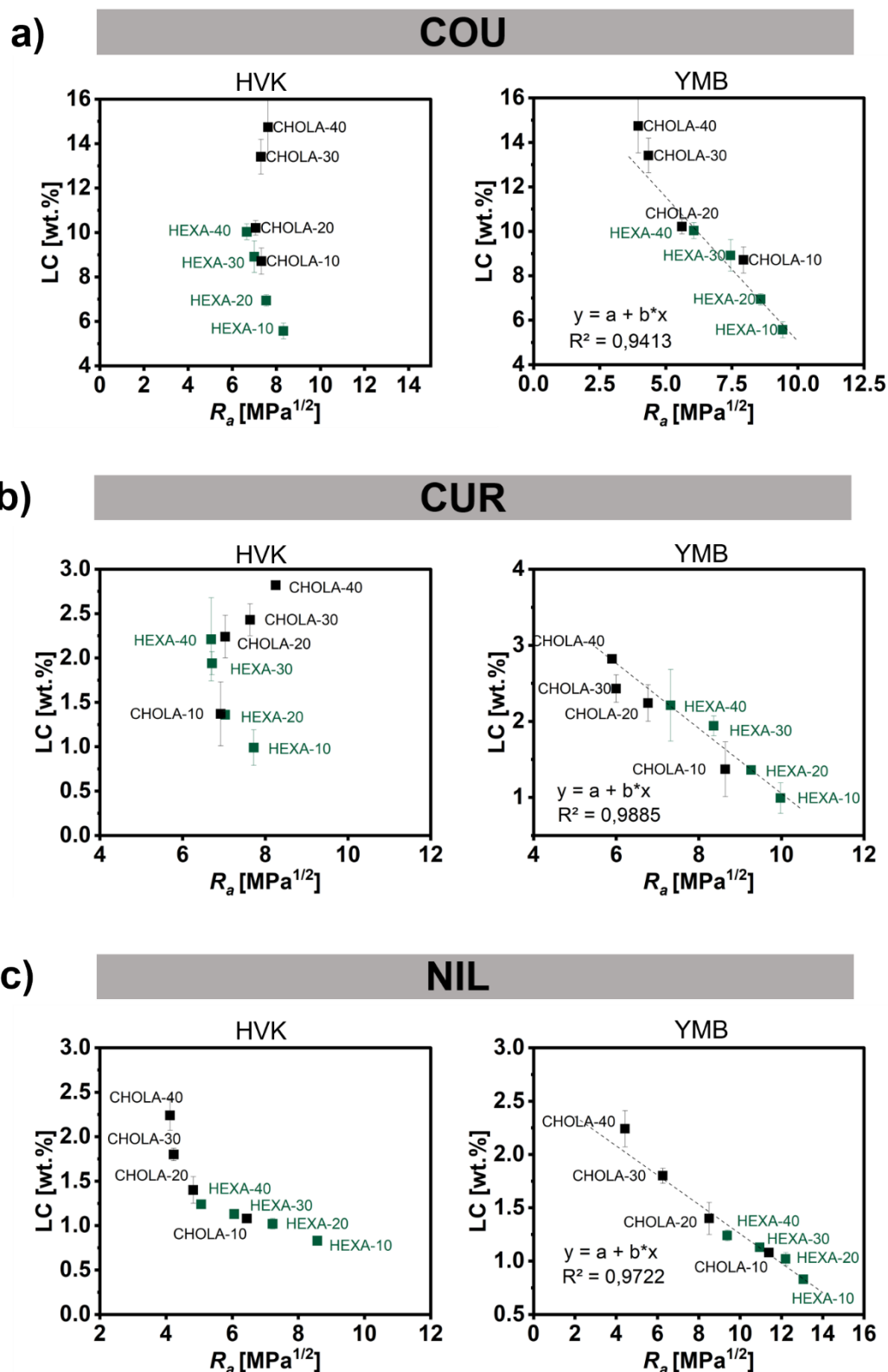


Figure S26. χ values of the HEXA-10 to 40 (green color) and CHOLA-10 to 40 (black color) particles with coumarin (a), curcumin (b) and Nile red (c) calculated by HVK method in correlation with LC determined by co-solvent loading method.

5.3 Influence of hydrophobic content on the correlation between R_a and cargo LC (comparison of HVK and YMB method)



6. Part D: Integrating all correlations into a master curve as predictive model for cargo loading in amphiphilic nanogels

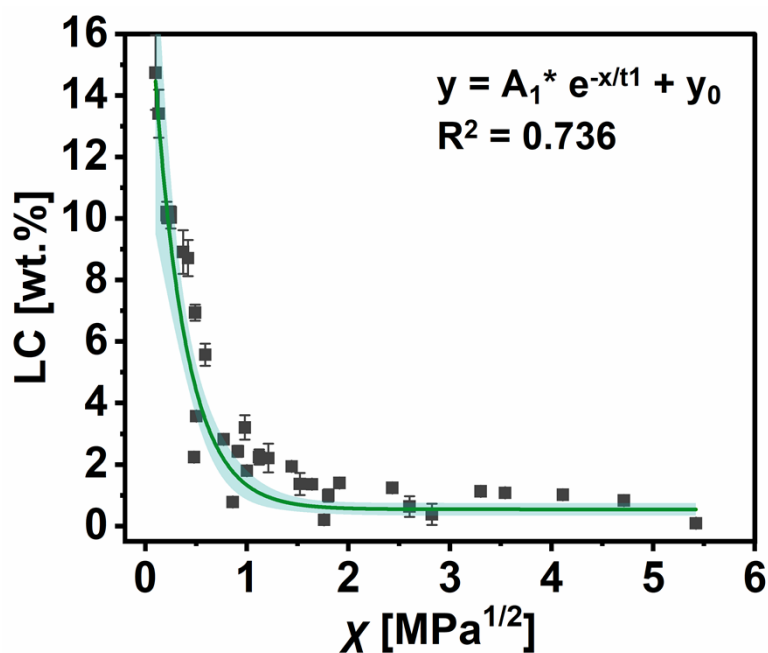


Figure S28. Correlation of LC with χ for all ANG-cargo combinations by an exponential fit. All χ values were calculated via the YMB method and LC was determined by co-solvent loading method.

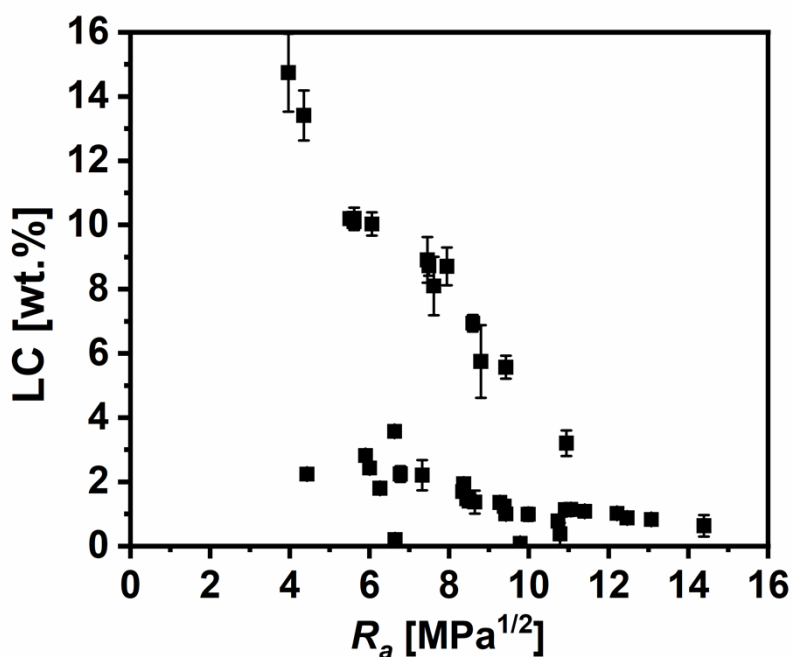


Figure S29. Correlation of LC with R_a for all ANG-cargo combinations. All R_a values were calculated via the YMB method and LC was determined by co-solvent loading method.

7. References

- 1 X. Farto-Vaamonde, G. Auriemma, R. P. Aquino, A. Concheiro and C. Alvarez-Lorenzo, *Eur. J. Pharm. Biopharm.*, 2019, **141**, 100–110.
- 2 HPLC Determination of Meloxicam on Newcrom R1 Column, <https://sielc.com/hplc-determination-of-meloxicam>.
- 3 Y. K. Han and A. I. Segall, *J. Chromatogr. Sci.*, 2015, **53**, 761–766.
- 4 M. V. Barbosa, L. O. F. Monteiro, A. R. Malagutti, M. C. Oliveira, A. D. Carvalho-Junior and E. A. Leite, *J. Braz. Chem. Soc.*, 2015, **26**, 1338–1343.
- 5 S. Wankhede, M. Tajne, K. Gupta and S. Wadodkar, *Indian J. Pharm. Sci.*, 2007, **69**, 298.
- 6 D. W. Van Krevelen and K. Te Nijenhuis, in *Properties of Polymers*, Elsevier, 1997, pp. 189–227.
- 7 R. F. Fedors, *Polym. Eng. Sci.*, 1974, **14**, 147–154.
- 8 C. M. Hansen, *J. Paint Technol.*, 1967, **39**, 104–117.